Fuel Processing Technology 274 (2025) 108240

Contents lists available at ScienceDirect

Fuel Processing Technology

journal homepage: www.elsevier.com/locate/fuproc

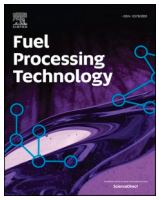

The co-combustion and pollutant emission characteristics of lignite and lake sediment

Xinyu Zheng [a,b], Manxia Shang [a], Bowen Zhang [c], Yunmei Li [a], Suilin Wang [b], Zhong Huang [a,*]

[a] Key Laboratory of Thermal Science and Power Engineering, Department of Energy and Power Engineering, Tsinghua University, Beijing 100084, China
[b] School of Environmental and Energy Engineering, Beijing University of Civil Engineering and Architecture, Beijing 100044, China
[c] School of Human Settlements and Civil Engineering, Xi'an Jiaotong University, Xi'an 710014, China

ARTICLE INFO

Keywords:
Co-combustion
Lake sediment
Lignite
Pollutant emission
Circulating fluidized bed boiler

ABSTRACT

Lake sediment is a high moisture solid waste that carries a large amount of water pollutants, significantly impacting the environment and urban landscape. The efficient management of lake sediment has emerged as a critical challenge requiring immediate attention. This paper focuses on the characteristics of co-combustion and its pollutant emissions. The combustion characteristics of mixed combustion of lake sediment and coal in different proportions were obtained by the thermogravimetric method. Experiments elucidated the influence of diverse factors on the variability of NO and SO_2 concentrations. The remaining bottom residue of the reaction and the reasons for the changes in emission concentration are analysed from a microscopic perspective. Results indicate that the appropriate proportion (<20 %) of mixed lake sediment promotes coal combustion. NO and SO_2 decrease with increased bed temperature, lake sediment mixing ratio (5 %–15 %), and particle size. As the bed temperature increases, the particle surface melts, reducing the pore structure and reaction sites, thereby reducing the generation of pollutants. When the mixing ratio exceeds 15 %, NO increases while SO_2 decreases. Calcium based substances have little catalytic effect on NO, but are still effective for SO_2. Larger particles will promote the decomposition of NO on their surface.

1. Introduction

Solid waste is ubiquitous in industrial processes, and its harmless disposal is still a topic of heated debate [1,2]. Incineration disposal is currently the most commonly used disposal method [3], which has problems of high energy consumption, emissions, and costs [4]. Circulating fluidized bed boilers provide an effective option for burning solid waste due to their wide fuel adaptability and low combustion temperature [5]. Various experimental studies and operational experience have shown that co-combustion coal can recover solid waste instead of dedicated incinerators, thereby achieving higher energy conversion efficiency and reducing costs [6]. That achieves higher energy conversion efficiency and reduces costs [7]. This method has significant advantages in treating solid waste with high moisture content and low calorific value [8].

Co-combustion methods have significant advantages in improving combustion efficiency. Thermogravimetric analyser (TGA) experiments have shown that adding biomass can improve the combustion efficiency of coal. The comprehensive combustion index (S) of the mixed sample is better than that of coal burned alone [9]. However, the change in the comprehensive combustion index does not have a linear relationship with the mixing ratio [10].

The cooperation of fuel and solid waste can also reduce pollutant emissions. Miao et al. [11] mixed various materials such as red mud with coal and burned them in a CFB boiler, which had a slight impact on NO. Among them, the impact of red mud was the most significant. Liu et al. [12] mixed organic solid waste with lignite for combustion. Comprehensive analysis showed that the mixing ratio should not exceed 30 %. Gu et al. [13] found that synergistic treatment of sludge under high temperature and low oxygen conditions can significantly reduce nitrogen oxide emissions. However, the co-combustion of sludge and coal at high mixing ratios has a limited impact on pollutant emissions. If the combustion is stable, a high proportion (50 %) of mixed combustion can be achieved [14]. In addition, adding adhesives can also reduce the emission of pollutants for various solid waste mixed samples and coal co-combustion [15]. Ż Ukowski et al. [16] found that the addition of mixed samples can reduce the emission factor by creating a bubble coalescence environment during combustion in a fluidized bed boiler. Yang et al.

* Corresponding author.
E-mail address: huangzhong@tsinghua.edu.cn (Z. Huang).

https://doi.org/10.1016/j.fuproc.2025.108240
Received 20 March 2025; Received in revised form 14 May 2025; Accepted 20 May 2025
Available online 31 May 2025

[17] mixed sludge with biomass, and nitrogen oxide emissions decreased as the proportion of sludge increased. Huo et al. [18] mixed coal gangue with biomass at a ratio of 20 % and found that it can promote combustion and reduce NO emissions. In addition, co-combustion of biomass and coal can reduce carbon dioxide emissions [19].

Lake sediment falls under the category of sludge. It is characterized by high water content, low calorific value, and the challenge of being difficult to incinerate on its own. Co-combustion with coal is an effective method to improve system stability and thermal efficiency [20]. Lignite has a high production volume but poor coal quality and high transportation costs, significantly affecting its utilization rate. Co-combustion of lignite with lake sediments from the same region will address the issue of low lignite utilization. This approach alleviates lake sediments' disposal pressure, promotes resource utilization, and supports environmental protection. Previous studies on the co-combustion of solid waste and lignite have shown that mixing other solid waste can improve the combustion performance [9]. As the mixing ratio of solid waste increases [21,22], the conversion rates of NO and SO_2 decrease. Excessive mixing ratios can increase the conversion rate of HCl, leading to an increased risk of corrosion. Therefore, selecting an appropriate mixing ratio provides significant assistance and guidance for practical applications.

The purpose of this study is to confirm that lake sediments can be used as combustion fuels and find the appropriate mixing ratio. Taking Dianchi Lake sediments as the research object, the combustion characteristics of lake sediments and lignite co-combustion under different ratios are analysed. The pollutant emission characteristics under the influence of bed temperature, particle size, and mixing ratio are investigated. We also observed the surface morphology and composition of the lake sediment and lignite mixture after combustion to explore the mechanism of pollutant generation. Propose the optimal co-combustion ratio that balances combustion and emission performance, and analyse the influencing factors from a mechanistic perspective. Providing reference for practical engineering applications is significant for the utilization and disposal of sediment resources in lakes such as Dianchi Lake.

2. Materials and methods

2.1. Materials characteristics and preparation

The lake sediment was taken from Dianchi Lake in Yunnan Province, China, and the lignite was taken from Xiaolongtan in Yunnan Province. The lake sediment undergoes preliminary drying at the sewage-treatment plant. Lake sediments and lignite are dried in a dryer at 105 °C for 2 h and stored in a sealed container. Simultaneously, grinding and sieving operations on the dried lake sediments and lignite will be conducted to obtain more accurate and uniform particle sizes. A small portion of lake sediment and lignite was extracted separately. These samples were then subjected to a vibrating screen machine to separate them into materials with a diameter of less than 0.075 mm. Subsequently, the separated materials were burned in a muffle furnace to prepare ash samples for further analysis by X-ray Fluorescence (XRF) and X-Ray Diffraction (XRD). The remaining lake sediments were sieved using different mesh sizes to obtain samples with particle sizes of 0.2 mm–0.4 mm, 0.4 mm–0.6 mm, and 0.6 mm–0.8 mm. And the remaining lignite was sieved using a vibrating screen to obtain samples with particle sizes ranging from 0.4 mm to 0.6 mm. The lake sediments with varying particle sizes were mixed lignite of equivalent size in specific proportions of 5 %, 10 %, 15 %, 20 %, and 30 %. Subsequently, seal the processed material for future utilization. Before the experiment, an electronic balance (The measurement accuracy is 0.0001) was used to weigh a total of 0.1 g of mixed material, placing it into the feeding device, and 1 g of quartz sand with a particle size of 0.3 mm as the reaction bed material. The N_2 and O_2 used in the experiment are standard gases with a concentration of 99 %.

Industrial and elemental analysis of the materials was conducted using XRD and XRF. The results of the study of physical and chemical properties are shown in Table 1. Lake sediments exhibit a low calorific value, fixed carbon content, and high ash content. Table 2 shows that the lake sediment mainly contains four types of oxides: SiO_2, Al_2O_3, CaO, and Fe_2O_3.

Fig. 1 shows the derivative peaks obtained from XRD analysis of lake sediments and lignite using an X-ray diffractometer.

2.2. Experimental procedures

Thermogravimetric analysis (TGA) was conducted using a comprehensive STA449F3 thermal analyser. Eight micrograms of material were used for each experiment. The experiment was conducted at air atmosphere conditions and a termination temperature of 1000 °C(with a heating rate of 10/20/30 °C/min). TG-DTG (Thermogravimetry-Differential Thermogravimetry) curves were obtained at mixing ratios of 10 %, 20 %, and 30 % of lake sediment and coal.

The co-combustion pollutant measurement experiment was conducted in a tubular furnace. The experimental setup mainly consists of a tubular furnace, a quartz tube reactor (furnace section), a feeding system, a gas supply system, a flow control system, and a flue gas detection system, as shown in Fig. 2.

The furnace simulates the residence time and temperature characteristics in a small circulating fluidized bed boiler, with the mixed samples undergoing reactions in the fluidized reaction zone. The valve switches located on the connecting pipes can be used to detect the airtightness of the system separately. The gas is exhausted from the system, and nitrogen is introduced to maintain an inert atmosphere, minimizing co-combustion reactions in the mixed sample as it enters the reaction zone. The minimum fluidization airflow rate (6 L/min) was obtained through cold state experiments using an experimental system. This indicates that 1.26 L/min of oxygen and 4.74 L/min of nitrogen must be introduced during the reaction to ensure the bed material remains fluidized and to simulate the combustion reaction in a circulating fluidized bed boiler. Prior to each test, the analyser is calibrated with standard gas.

In circulating fluidized bed boilers, the location and method of feeding significantly affect pollutant emission characteristics [23]. Therefore, a feeding system was designed to ensure consistency in every feeding position and method. The feeding system operates by feeding materials from above the quartz tube. Once the preset reaction temperature reaches the furnace, nitrogen gas is introduced at a rate of 6.5 L/min, propelling the pre-placed materials into the feed tube and reactor. Immediately following this introduction, the feed gas valve is swiftly closed to prevent excessive nitrogen from entering and disrupting the reaction gas ratio. The gas supply system then introduces a premixed combination of nitrogen (79 %) and oxygen (21 %) into the reactor, creating an air atmosphere. Before reaching the reaction temperature, a brief introduction of nitrogen is carried out to maintain an inert environment within the reactor.

2.3. Analytical methods and data processing

Thermogravimetric experiments obtained the TG-DTG curves of two samples at mixing ratios of 10 %, 20 %, and 30 %. The comprehensive and combustible characteristics indexes were calculated, the theoretical and experimental values of weight loss and weight loss rate were compared, and the influence of lake sediment mixing on lignite combustion was analysed.

Build a bubbling bed reactor and measure the trend of pollutant emission concentration by changing the bed temperature (700 °C,750 °C,800 °C,850 °C,900 °C), mixing ratio (5 %,10 %,15 %,20 %,30 %), and fuel particle size (0.2 mm–0.4 mm,0.4 mm–0.6 mm,0.6 mm–0.8 mm). SEM-EDS analysis was conducted on the bottom slag to obtain mineral composition, oxide, and elemental composition, and

Table 1
Industrial and elemental analysis of sediment in Dianchi Lake and Xiaolongtan lignite.

Materials	M_{ar} (%)	A_{ar} (%)	V_{ar} (%)	FC_{ar} (%)	C_{ar} (%)	H_{ar} (%)	O_{ar} (%)	N_{ar} (%)	S_{ar} (%)	$Q_{net,\ ar}$ (MJ/kg)
Lake sediment	**6.70**	66.30	25.10	1.80	12.74	2.22	11.07	0.66	0.31	4.74
Lignite	**20.15**	17.90	31.80	30.15	43.22	4.95	10.80	0.95	2.04	17.11

Table 2
XRF analysis of Dianchi Lake sediment and lignite.

Materials	SiO_2 (%)	Al_2O_3 (%)	CaO (%)	Fe_2O_3 (%)	K_2O (%)	TiO_2 (%)	SO_3 (%)	MgO (%)
Lake sediment	50.16	19.32	14.43	7.47	3.19	1.91	1.75	1.51
Lignite	35.54	29.14	10.58	8.84	0.91	1.31	11.78	1.28

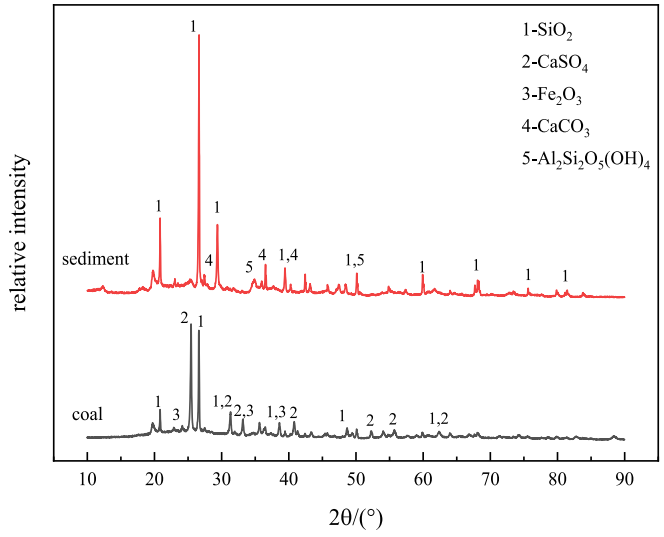

Fig. 1. XRD analysis of Dianchi Lake sediment and lignite.

further analysis was conducted on the changes in pollutant emissions from a microscopic perspective.

In thermogravimetric experiments, it is impossible to compare the combustion characteristics of a specific reaction stage with other substances due to the different reaction processes and stages of different materials. Therefore, the comprehensive combustibility index (S_N) and combustion index (C) are introduced to calculate and compare the combustion characteristics according to Eq. (1) and Eq. (2) [24–26].

$$S_N = \frac{\left(\frac{dw}{dt}\right)_{max}\left(\frac{dw}{dt}\right)_{mean}}{T_i^2 T_b} \tag{1}$$

$$C = \frac{\left(\frac{dw}{dt}\right)_{max}}{T_i^2} \tag{2}$$

where $(dw/dt)_{max}$ is the maximum combustion rate,%/min, $(dw/dt)_{mean}$ is the average combustion rate,%/min, T_i is the ignition temperature, K, T_b is the burnout temperature.

Introduce theoretical calculation values for weight loss and weight loss rate, and use the deviation between experimental and theoretical values to describe the impact of synergistic effects on the combustion stage. Calculate the theoretical value according to Eq. (3) [27].

$$W_{\text{theoretical}} = x_1\left(\frac{dw_1}{dt}\right) + x_2\left(\frac{dw_2}{dt}\right) \tag{3}$$

where x_1 is the mass fraction of lignite in the mixed sample, w_1 is the weight loss rate of coal during single combustion, x_2 is the mass fraction of sediment in the mixed sample, w_2 is the weight loss rate of sediment during single combustion.

In the pollutant determination experiment, emissions are mainly concentrated in the first 3 min of the combustion process. Emission data were selected during this period to analyse the primary pollutants NO and SO_2 in flue gas. The instantaneous concentration curves of two gases

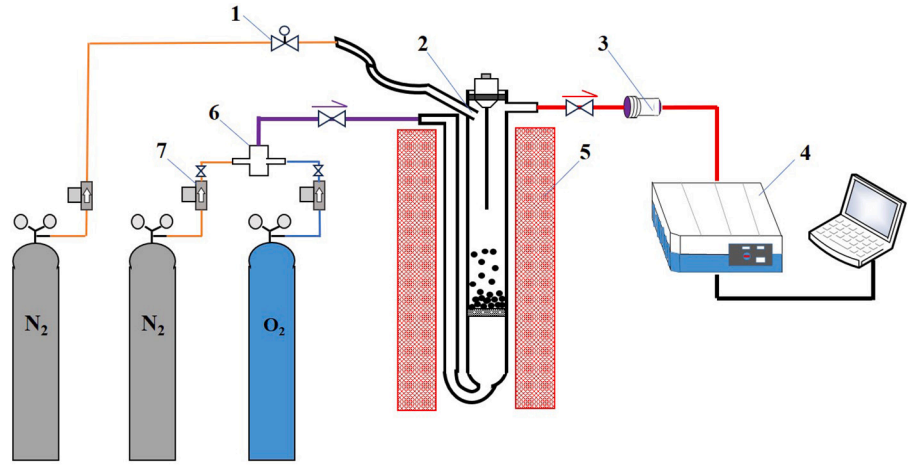

1: three-way valve; 2: feed port; 3: Filter cartridge; 4: flue gas analyzer; 5: Tube Furnace; 6: gas mixer; 7: Gas flow meter

Fig. 2. Experimental system flowchart.

were obtained from the experiment. The total emissions can be estimated by integrating the release curves of SO_2 and NO gases.

The nitrogen oxide conversion rate of fuel under different operating conditions can be calculated through experiments, which characterizes the NO generation during the combustion of coal particles. The combustion characteristics, according to Eq. (4).

$$\eta = \frac{M_N}{m_N} \times \frac{\int_{t2}^{t1} c dt}{22.4 \times 6 \times 10^7} \times 100\% \quad (4)$$

where η is nitrogen oxide conversion rate, %, m_N is mass of nitrogen in flue gas, g, M_N is molar mass of nitrogen atoms, g·mol^{-1}, Q is total gas volume flow rate, L·min^{-1}, C is Instantaneous volumetric concentration of nitrogen oxides at a certain moment, $\mu L \cdot L^{-1}$, t_2-t_1 is Time required for complete combustion of the experimental materials, s.

In the SEM-EDS (Scanning Electron Microscope-Energy Dispersive Spectrometry) experiment, the bottom residue after the reaction is screened out, and the sample adheres to an aluminium disk with double-sided copper tape for detection. The apparent morphology is observed by magnifying it 500, 1000, and 2500 times, respectively. Representative areas are selected to obtain energy spectrum data, and the types and contents of metallic elements in the solid residue are determined.

3. Results and discussions

3.1. Effect of co-combustion properties

TG-DTG curves of lake sediment single combustion and co-combustion in different proportions are shown below.

As shown in Fig. 3, the TG curves for the combustion of pure coal and different blending ratios are presented. According to the inflection points in the figure, there are mainly four stages of blended combustion: water evaporation, volatile matter release, secondary volatile matter release, and fixed carbon combustion. The low-temperature combustion stage occurs between 220 and 420 °C. During this stage, a lot of volatile matter is released from the mixed samples. Fixed carbon combustion also takes place during this stage. Between 420 and 600 °C, secondary volatile matter and coke in the mixed samples undergo combustion. The TG curve is smoother in this stage compared to the previous one.

As shown in Fig. 4, the DTG curves for the combustion of pure coal and different blending ratios are presented. Compared to coal combustion alone, co-combustion results in greater total weight loss and a more significant reduction in the maximum weight loss rate during the low-temperature combustion stage. As the blending ratio increases, weight loss decreases, the maximum weight loss rate slightly diminishes, and the maximum peak shifts slightly to the right. In the high-temperature stage, the peak of the DTG curve decreases with increasing blending ratio. The weight loss of pure coal is less than that of coal mixed with bottom ash. This may be because as the temperature rises, the decomposition of complex organic compounds present in the bottom ash intensifies, breaking down larger organic molecules into smaller volatile compounds, thereby exacerbating the mass loss [28].

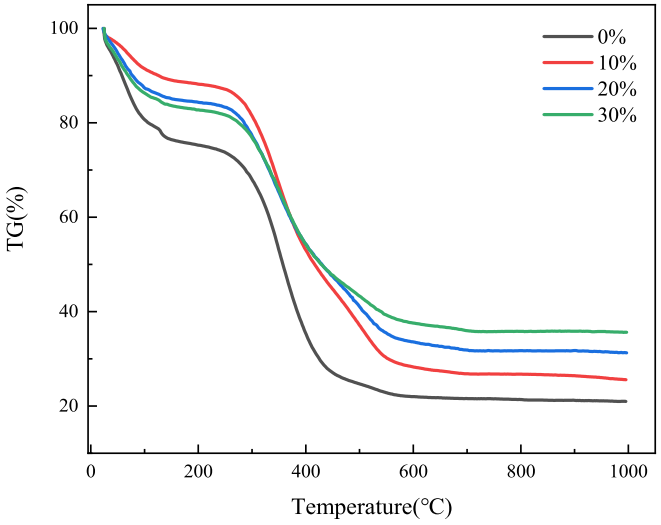

Fig. 3. TG curve under different ratios of bottom mud and lignite blending.

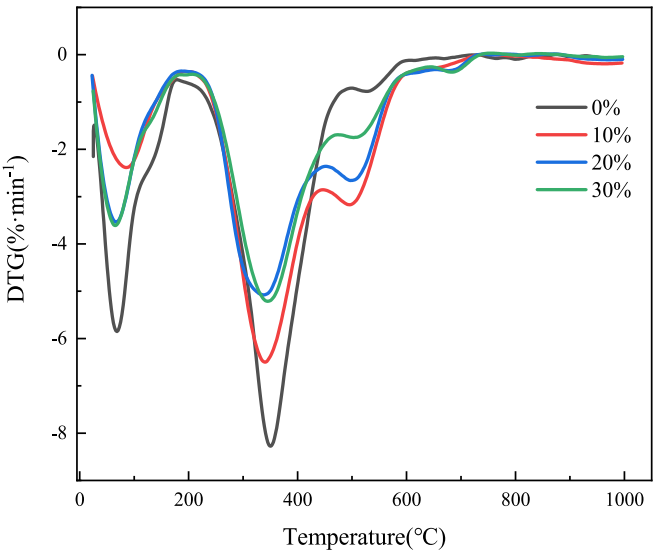

Fig. 4. DTG curves under different ratios of bottom mud and lignite blending.

Draw a TG curve based on calculated values and experimental data, obtain a DTG curve through first-order differentiation, and explore the differences between them.

As shown in Fig. 5, the theoretical experimental comparison of TG and DTG at mixing ratios of 10 %, 20 %, and 30 % is presented. The differences between the calculated and experimental values of TG and DTG shown in the figure indicate the existence of interactions between the bottom ash and lignite during the combustion process [29].

The final residual mass increases with the higher proportion of sediment admixture for the TG curve. Under the mixing conditions of 10 %, 20 %, and 30 %, the experimental residual masses are all no higher than the calculated values, indicating that interactions positively affect the burnout characteristics of the material. This may be due to the high ash content in the sediment and the presence of catalytic metal oxides in the ash, which facilitate coke combustion [26].

For the DTG curve, in the first stage of the reaction, the experimentally measured peak is lower than the theoretically calculated peak, suggesting that the interaction of the mixture inhibits water evaporation. In the second stage, the ash content rises as the mixing ratio increases, leading to reduced weight loss. This may be due to the initial precipitation of easily decomposable volatiles in the sediment, which blocks the gaps between the samples, preventing timely oxygen diffusion into the blend. In the third stage, the experimentally measured peak is significantly greater than the theoretically calculated one. It can be inferred that a smaller portion of the secondary volatiles rapidly evaporates and precipitates into the pores of the residual coal carbon, allowing complete combustion reactions with oxygen, resulting in experimental values higher than theoretical values [30].

C and S_N represent comprehensive characteristics of ignition and the entire combustion process. Based on the data obtained from thermogravimetric experiments, use Eqs. (1), (2) to calculate the values of C and S_N at different mixing ratios.

Table 3 shows comprehensive combustion characteristics (S_N) and combustible characteristics (C) under different mixing ratios by calculation. The ignition temperature increases with the blending ratio

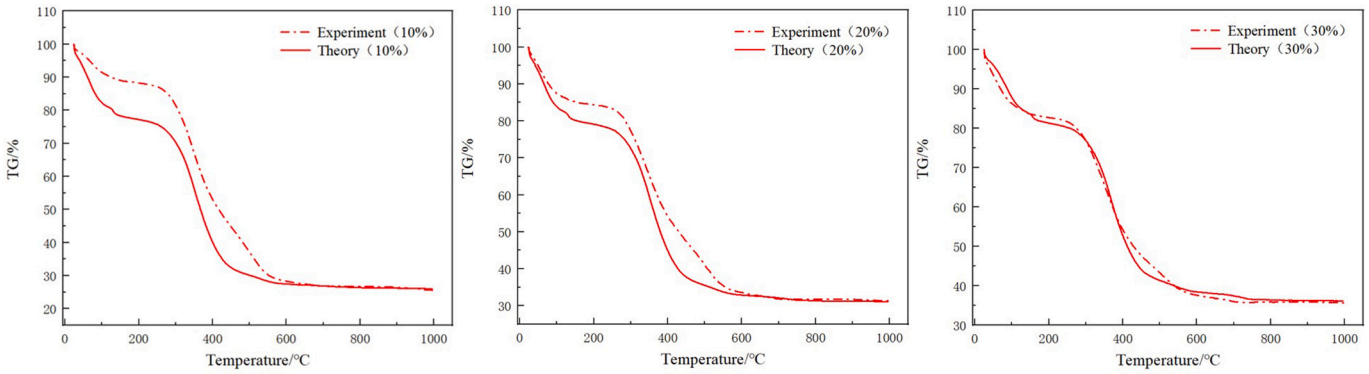

a）Comparison chart of TG theory and experiment at mixing ratios of 10%, 20%, and 30%

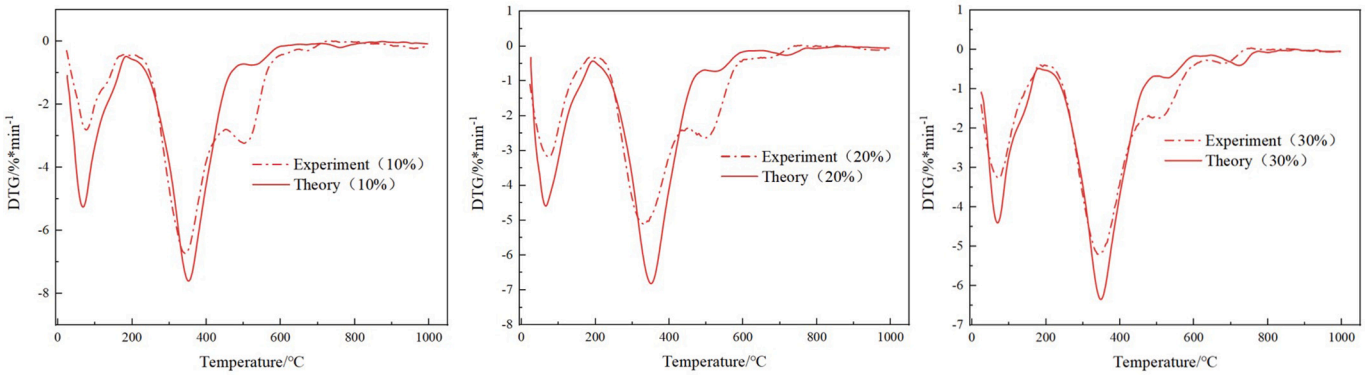

b）Comparison chart of DTG theory and experiment at mixing ratios of 10%, 20%, and 30%

Fig. 5. Comparison of TG and DTG theoretical experiments at mixing ratios of 10 %, 20 %, and 30 %. a) Comparsion chart of TG theory and experiment at mixing ratios of 10 %, 20 %, and 30 %. b) Comparsion chart of DTG theory and experiment at mixing ratios of 10 %, 20 %, and 30 %.

Table 3
Related data on combustion characteristics under different mixing ratios.

Mixing ratios	DTG_{max}	Average of DTG	T_i	T_b	T_{max}	S_N	C
%	%·min^{-1}	%·min^{-1}	°C	°C	°C	10^{-7}	10^{-5}
0	−8.40 %	−0.049	248.7	441.5	347.34	150.73	13.58
10	−6.28 %	−0.040	245.4	741.3	313.6	61.76	8.28
20	−5.90 %	−0.033	257.3	746.7	319.7	49.69	8.36
30	−5.94 %	−0.030	258.1	743.9	331.2	43.58	7.76

increase, and the burnout temperature change is insignificant. The comprehensive combustion characteristic index shows a sharp increase at a 30 % blending ratio, and coal begins to play a certain role.

With an increase in the mixing ratio, the combustible characteristic index rises, and the ignition performance improves, indicating that blending a certain amount of sediment can enhance the ignition performance of coal, facilitating stable combustion. Scholars studying the co-firing of biomass and coal have found that, due to the presence of easily decomposable and ignitable components, biomass releases heat at the initial stage of ignition, serving to preheat the coal and promote the evaporation of volatile substances in the coal, which is beneficial for the ignition and stable combustion of coal. Similarly, with a low ignition temperature, sediment can also preheat the coal at the initial combustion stage [31].

As shown in Fig. 6, the comprehensive combustion index decreases with increasing mixing ratio, and the index significantly drops when the ratio reaches 30 %. This is due to the low ignition temperature Ti of the sediment and the high burnout temperature of coal. When they are co-fired, the reaction process becomes longer, and the combustion intensity relatively weakens [32]. Therefore, an excessively high blending ratio is not conducive to improving the combustion performance of the fuel.

3.2. *Effect of bed temperature on pollutant emissions*

Draw curves based on changes in pollutants at different temperatures.

As shown in Fig. 7, temperature affects the peak position of the NO concentration curve. With increasing temperature, the peak occurrence time advances slightly, and the peak value significantly decreases within the range of 750 °C–850 °C. This is because an increase in temperature accelerates the combustion rate and provides energy for NO_x formation earlier, although its impact is not significant [33]. There is no clear pattern in the bed temperature's effect on the peak of the SO_2 concentration curve; at 900 °C, the peak value is much higher than at other temperatures.

Integrate the instantaneous concentration to obtain the emission concentration under each operating condition and calculate the N

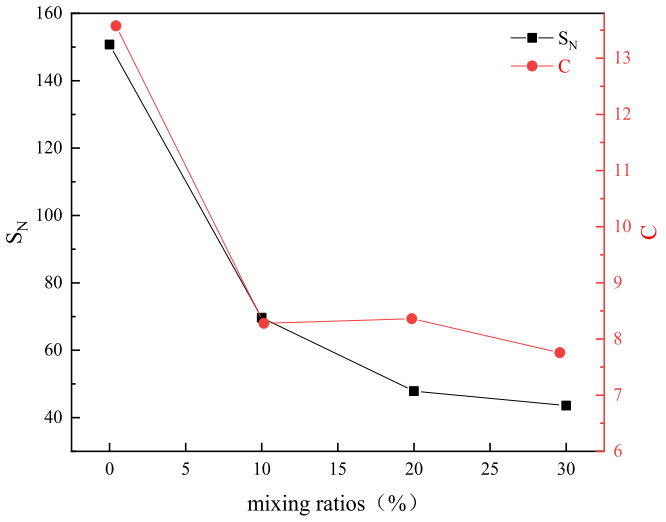

Fig. 6. Co-combustion characteristics of 10 %, 20 %, and 30 %.

conversion rate.

As shown in Fig. 8. the total NO emissions decrease significantly with temperature, with a significant decrease of 802.5 ppm at 800 °C and a minimum of 695.5 ppm at 900 °C. The change in total SO_2 emissions is insignificant in the low-temperature range, with minimal emissions at 900 °C. Integration reveals a downward trend in total NO emissions with increasing temperature. At 800 °C, a significant reduction to 50.56 ppm is observed, with the lowest point at 900 °C at 50.31 ppm. This is attributed to Eq. (4), where higher bed temperatures enhance both the rate of C—N conversion to NO_x and the reduction rate of NO_x. The greater reduction rate of NO_x leads to decreased NO_x emissions.

Based on the data obtained above, the total emissions of NO show a decreasing trend with increasing temperature. This is because, according to reaction Eq. (5) [34], the higher the bed temperature, the higher the rate of C—N conversion to NO_x and the reduction rate of NO_x. The higher the reduction rate of NO_x, the lower the NO_x emissions [34].

$$C(N) + NO \rightarrow N_2 + C(O) \quad (5)$$

Temperature has a significant impact on SO_2 emissions. As temperature rises, sulphur in the fuel becomes increasingly unstable, leading to the release and conversion of more sulphur into SO_2, thus increasing the emission concentration. Simultaneously, the sulphur fixation effect of alkali metal oxides diminishes, ultimately resulting in an increase in SO_2 concentration [35]. Analyse the reasons for the reduction of SO_2 emissions from a microscopic perspective using SEM.

As shown in Fig. 9, the observations of apparent morphology, suggest that after initial preheating, particle surfaces soften and become porous [36]. When temperature increases to a certain point, pore collapse and melting begin to occur, reducing the pore structure and making it difficult for sulphur to be released and converted into sulphur dioxide, leading to a decrease in SO_2 emissions [37].

3.3. *Effect of mixing ratio on pollutant emissions*

Draw curves based on changes in pollutants at different blending ratio. As shown in the Fig. 10, the trend of the peak instantaneous concentration of the two pollutants is completely consistent, and there is no significant change in the time of peak appearance. The maximum peak decreases with the increase of mixing ratio.

By integrating the instantaneous concentrations, we obtain the emission concentrations for each operating condition and calculate the nitrogen conversion rate.

As shown in the Fig. 11, the total emission concentration of NO

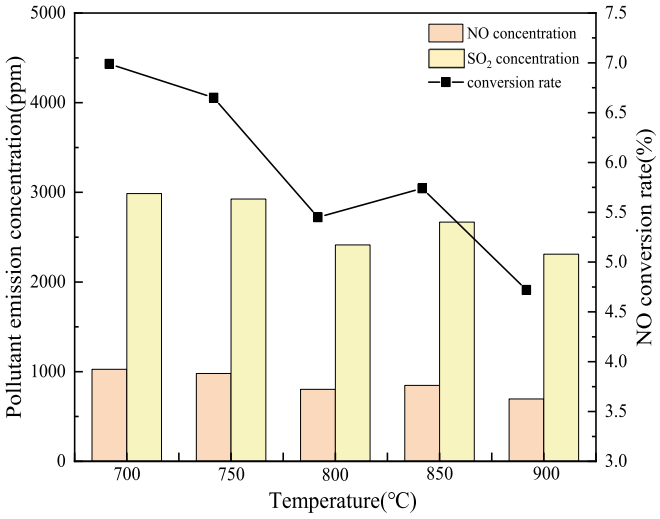

Fig. 8. Emission characteristics of pollutants at different bed temperatures.

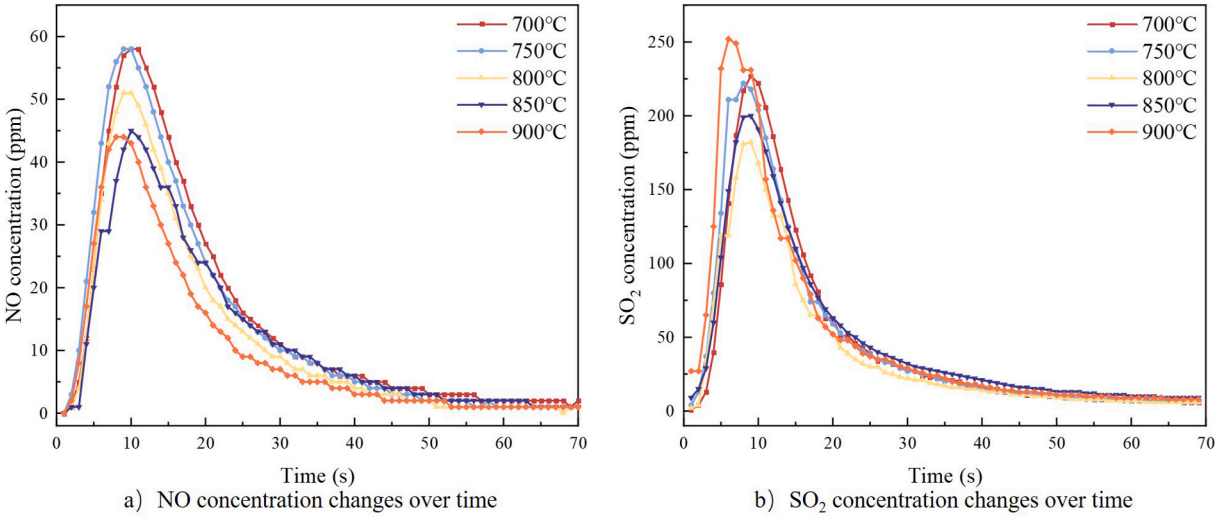

Fig. 7. Instantaneous variation of pollutant concentration at different bed temperaturesa)NO concentration changes over time; b) SO_2 concentration changes over time.

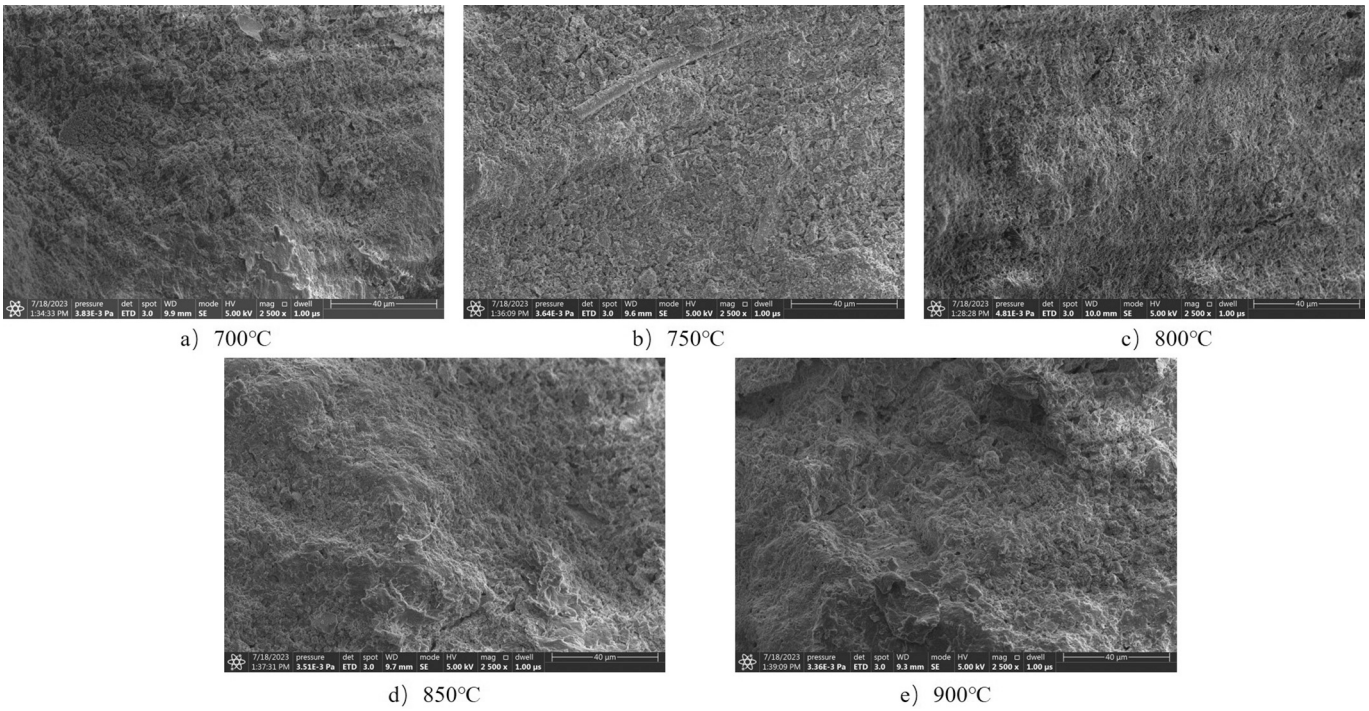

Fig. 9. Surface morphology of bottom slag at different bed temperatures (2500 times) a) 700 °C,b)750 °C,c)800 °C,d)850 °C,e)900 °C.

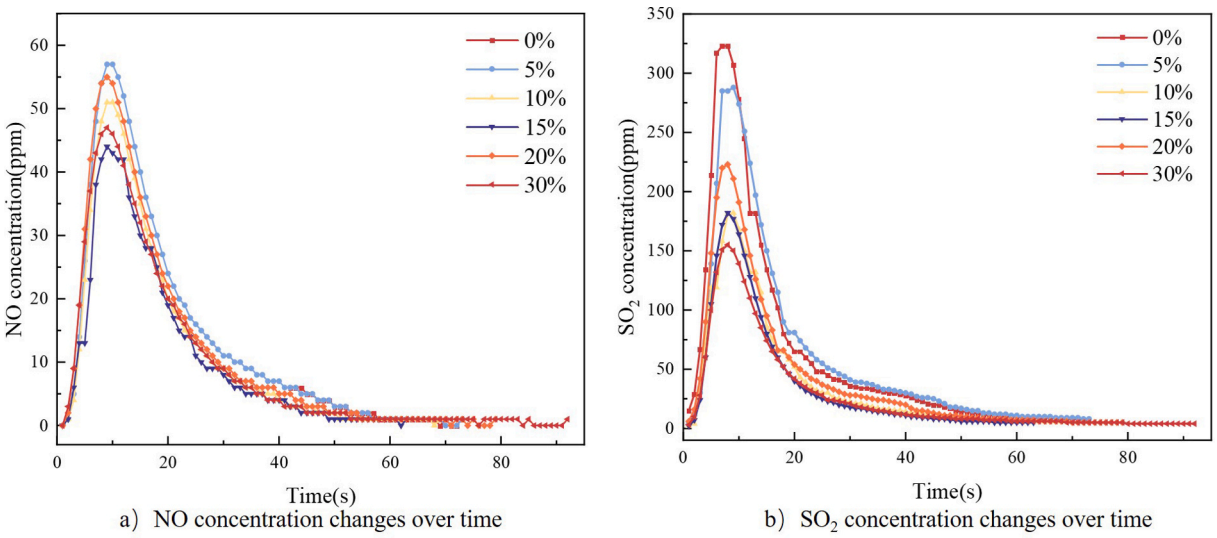

Fig. 10. Instantaneous variation of pollutant concentration with different mixing ratios a) NO concentration changes over time; b) SO_2 concentration changes over time.

decreases with the increase of blending ratio, and a turning point occurs when the ratio reaches 15 %. There is no obvious pattern, but the emission concentration is higher than that of pure coal, which is consistent with the conclusion obtained from combustion reaction. The emission of SO_2 mainly depends on the content of S in the fuel. With the addition of sediment, the emission concentration of SO_2 decreases, and it increases when the sediment mixing ratio reaches 20 %. The trend of N conversion rate is consistent with the change in total emission concentration. The lowest total NO emission occurs at a mixing ratio of 15 %, followed by a sharp increase. The lowest total SO_2 emission also occurs at a mixing ratio of 15 %.

Studies have shown [38] that the reaction between CO and SO_2 will compete with the reaction between CO and NO to reduce the conversion rate of NO. Some scholars [22,39] have also confirmed through experiments that alkaline earth metal compounds (CaO, MgO, etc.) as catalysts have good effects on suppressing pollutant emissions, and can react to generate sulphur and nitrates. Among them, calcium-based substances have a catalytic effect on NO production and an adsorption effect on sulphur. At the same time, fuels rich in calcium can reduce the maximum peak of NO gas emissions [40], and a large amount of calcium-based substances in the sample may increase N-NO conversion rate [41]. According to the XRF detection results in Section 2.1, there are 14.43 % CaO and 1.51 % MgO in the sediment, indicating that the catalytic effect of calcium based substances mixed more than a certain amount (>20 %) is not significant for NO, but still has a certain effect on SO_2.

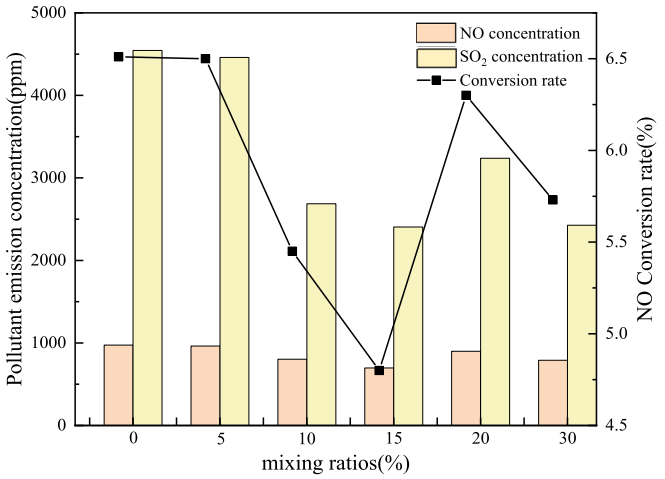

Fig. 11. Total emission concentration and conversion rate of pollutants with different mixing ratios.

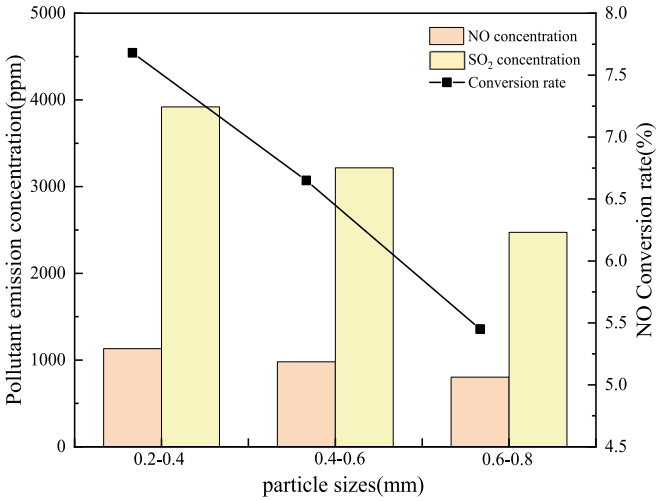

Fig. 13. Total emission concentration of pollutants with different particle sizes.

3.4. Effect of particle size on pollutant emissions

Draw curves based on changes in pollutants at different particle sizes. As shown in Fig. 12, with the increase of fuel particle size, the peak instantaneous concentrations of both pollutants decrease, and the peak appearance time lags slightly.

Integrate the instantaneous concentration to obtain the emission concentration under each operating condition and calculate the N conversion rate.

As shown in Fig. 13, the total emission concentrations of NO and SO_2 both decrease with the increase of fuel particle size, and the trend of N conversion rate change is consistent with the change of total emission concentration, with a similar decrease in magnitude.

Rahib et al. [42] found that the size of fuel particles affects the combustion process, making the flame more stable but increasing the amount of CO produced. Further research has shown [11] that larger coal particles increase the concentration of coal coke in the furnace, which is beneficial for the decomposition of NO*x* on the surface of coal coke.

3.5. SEM-EDS analysis

Select mixing ratios of 5 %, 15 %, and 30 % for pollutant concentration nodes, and observe the bottom slag under reaction conditions at 800 °C. Scanning electron microscopy (SEM) images of individual particle surfaces were magnified 2500 times, 1000 times, and 500 times, respectively.

As shown in Fig. 14, the surface of the bottom slag particles after mixed combustion is rough, with many isolated pores and cracks, and the crack distribution is uneven. When the mixing ratio is 5 %, there are more pores and uneven distribution. When the mixing ratio is 15 %, the gaps are relatively sparse. When the mixing ratio is 30 %, there are areas with dense cracks. Compared with the mixing ratios of 15 %, 5 %, and 30 %, the number of pores and gaps significantly increases, providing attachment points for the reaction element. Under these two mixing ratios, the concentration of pollutant emissions is higher.

Further, the sample was enlarged to 6500 times and representative regions were chosen to obtain the energy spectrum.

As shown in Fig. 15, the selected area mainly comprises O, Mg, Al, Si, Ca, and Fe elements. With the change of blending ratio, the mass proportion of Mg, Ca, and Si elements increases slightly, while the overall changes of other elements are not significant.

Under a 5 % mixing ratio of sediment, the surface morphology is not significantly changed, the surface remains rough, and there are irregular particles and pores on the surface. As the mixing ratio increases, the pores significantly decrease when the ratio reaches 15 %, and a small

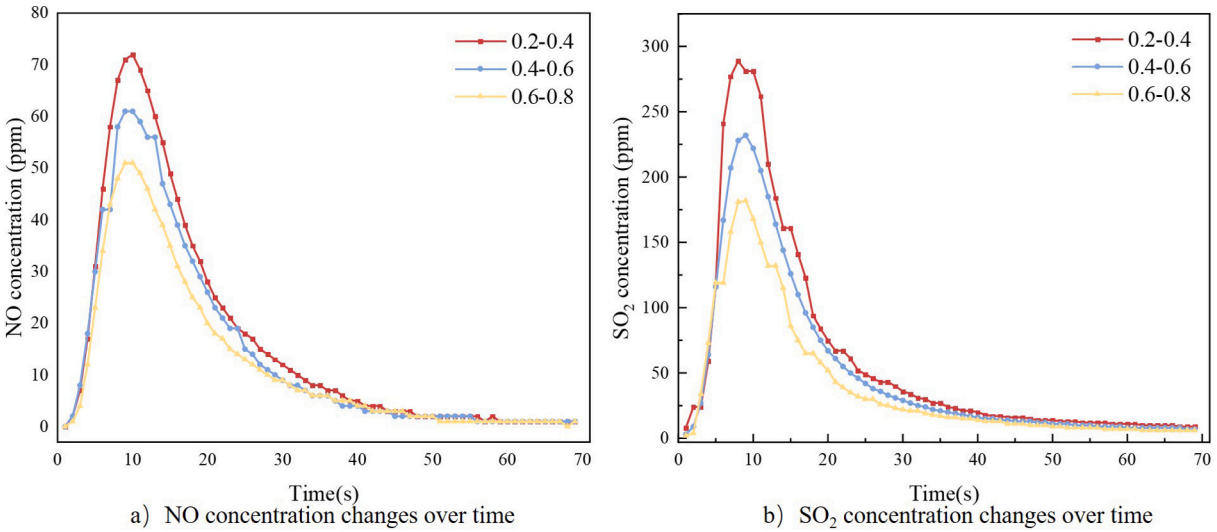

Fig. 12. Instantaneous variation of pollutant concentration with different particle sizes: a)NO concentration and b) SO_2 concentration changes over time.

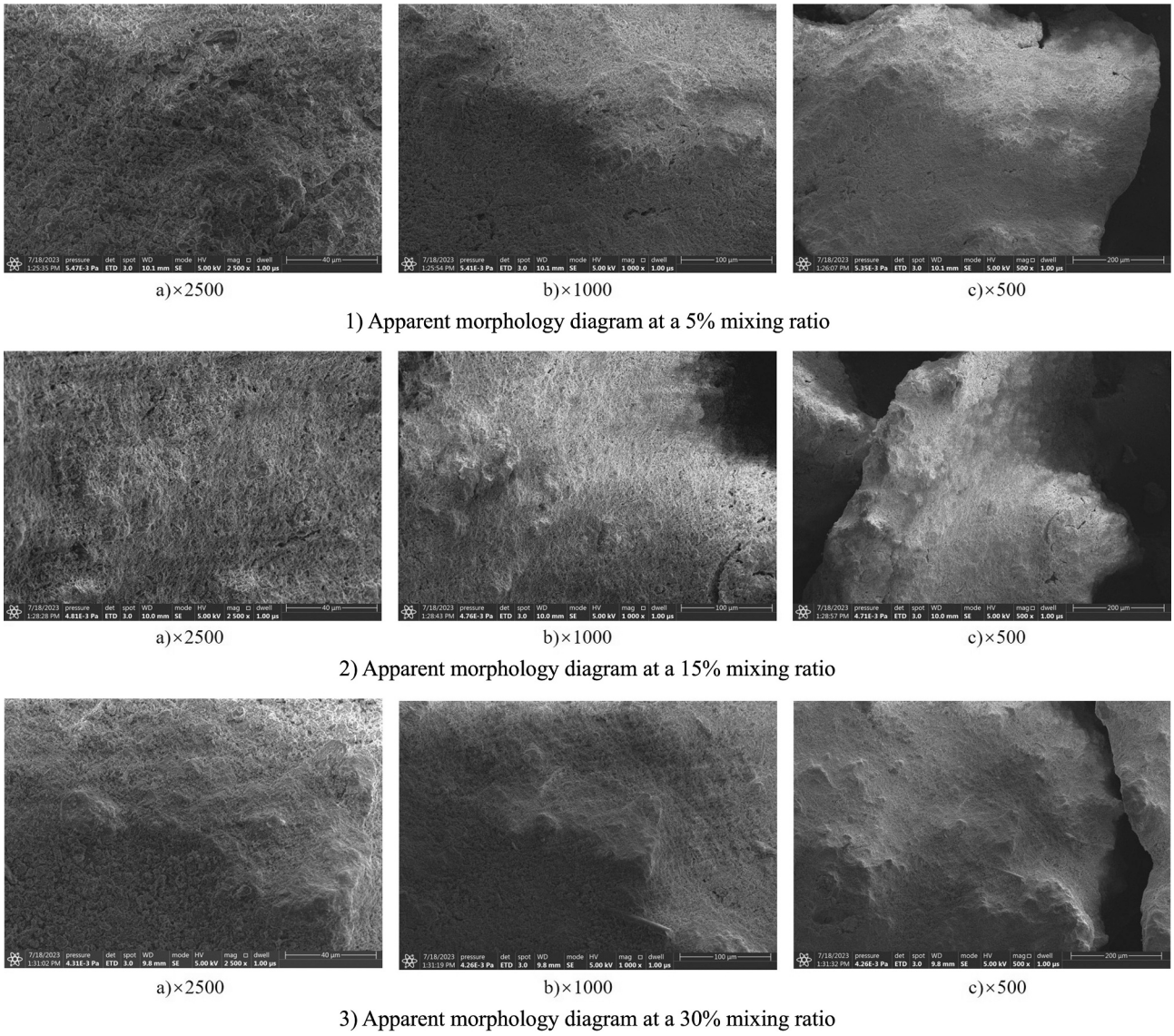

Fig. 14. Appearance diagram of 5 %, 15 %, and 30 % mixing ratios.
1) Apparent morphology diagram at a 5 % mixing ratio, 2) Apparent morphology diagram at a 15 % mixing ratio, 3) Apparent morphology diagram at a 30 % mixing ratio.

amount of molten crystals appear when the ratio reaches 30 %. According to previous scholars' research and EDS results, these crystals should be calcium silicoaluminate [35], which has a certain adsorption effect on nitrogen oxides.

4. Conclusions

This study obtained the optimal range of mixed combustion ratio between lake sediment and lignite to ensure economic and environmental protection and investigated the combustion characteristics and pollutant emission behavior of the Dianchi Lake sediment and the Xiaolongtan lignite at different temperatures, blending ratios, and particle sizes through thermogravimetric analysis and bubbling bed combustion experiments. This provides an effective and low-pollution approach for the comprehensive utilization of waste resources such as lake sediment. The main conclusions are as follows:

(1) There is a synergistic effect between the mixed combustion of lake sediment and lignite, and an appropriate blending ratio (<20 %) can improve the combustible characteristics of lignite.

(2) Raising the bed temperature effectively reduces the total emission concentration of NO and SO_2 pollutants, at 900 °C, the emission concentrations of NO and SO_2 are the lowest, at 695.5 ppm and 2310.5 ppm. The increase in temperature leads to an increase in the rate of C—N conversion to NO*x* and the reduction rate of NO*x*, thereby reducing NO emissions. It also increases the area of surface melting and collapse of fuel particles, reduces pore structure, and makes it difficult for S to be released and converted into sulphur dioxide, thus preventing a significant increase in SO_2 with the increase in S activity.

(3) By increasing the mixing ratio, the concentrations of NO and SO_2 show a decreasing trend. Compared to a mixing ratio of 5 %, at 15 %, the NO emission concentration decreased by 267 ppm and the SO_2 emission concentration decreased by 2055 ppm. However, after exceeding 20 %, the pollutant emission concentration increased. When the mixing ratio exceeds 15 %, the effect of calcium-based catalysts on N-NO conversion is insignificant. The alkali metal oxides in the lake sediment will no longer positively affect NO reduction, but there is still a certain adsorption effect

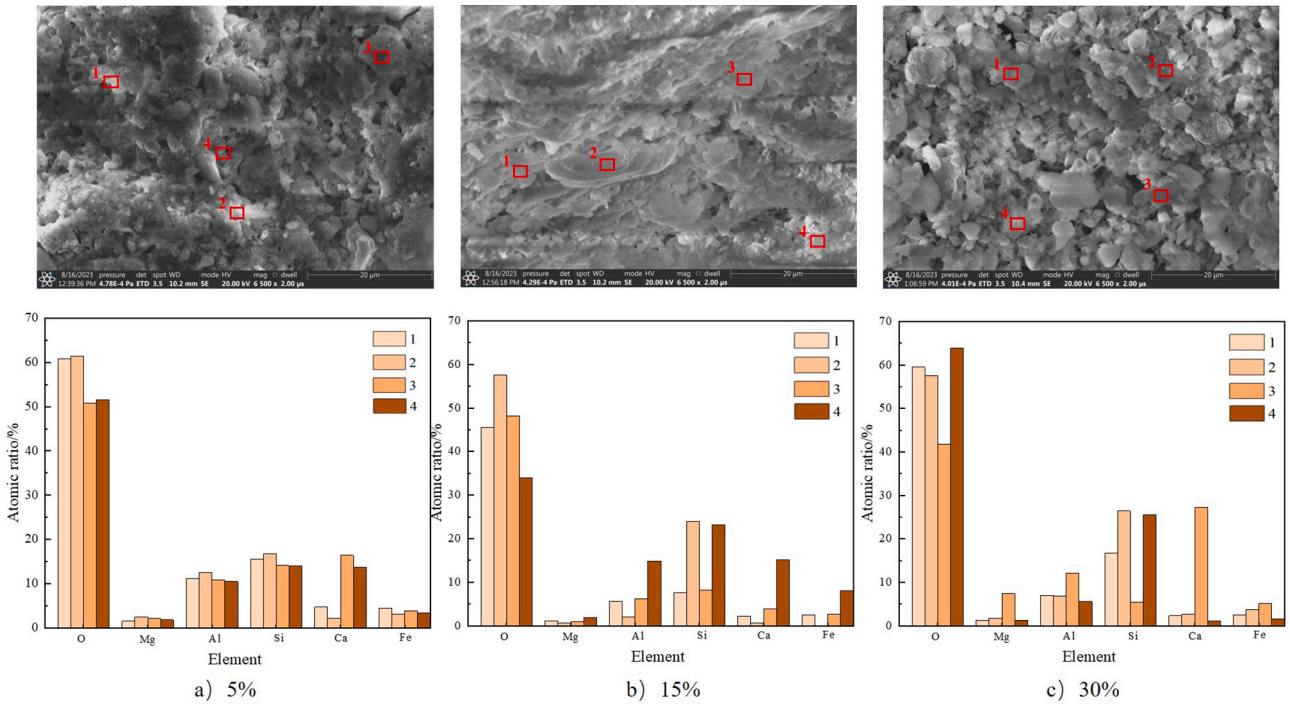

Fig. 15. SEM-EDS analysis at 5 %, 15 %, and 30 % mixing ratios (enlarged by 6500 times).

on SO_2. The mixing of lake sediment has a more significant impact on SO_2 than on NO.

(4) Increasing the fuel particle size results in a decreasing trend in the total emission concentrations of NO and SO_2. Larger particles are beneficial for the decomposition of pollutants on the surface of coal coke.

CRediT authorship contribution statement

Xinyu Zheng: Writing – original draft, Writing – review & editing, Conceptualization. **Manxia Shang:** Methodology, Writing – review & editing. **Bowen Zhang:** Writing – original draft, Writing – review & editing. **Yunmei Li:** Methodology. **Suilin Wang:** Supervision. **Zhong Huang:** Conceptualization, Project administration, Supervision, Methodology.

Declaration of competing interest

There are no actual or potential conflicts of interest including any financial, personal, or other relationships with other people or organizations within three (3) years of beginning the work submitted that could inappropriately influence (bias) their work.

Acknowledgment

This work is supported by Beijing Natural Science Foundation“Research on circulating fluidized bed combustion reconstruction method and resource utilization of high-aluminum coal ash” (JQ23010) .

Data availability

Data will be made available on request.

References

[1] M. He, F. Wu, G. Qu, X. Liu, Harmless and resourceful utilization of solid waste: multi physical field regulation in the microbiological treatment process of solid waste treatment, Environ. Res. 238 (2023) 117149, https://doi.org/10.1016/j.envres.2023.117149.

[2] H.-X. Zhao, F.-S. Zhou, A.L.M. Evelina, J.-L. Liu, Y. Zhou, A review on the industrial solid waste application in pelletizing additives: composition, mechanism and process characteristics, J. Hazard. Mater. 423 (2022) 127056, https://doi.org/10.1016/j.jhazmat.2021.127056.

[3] H. Liu, Y. Wang, S. Zhao, H. Hu, C. Cao, A. Li, Y. Yu, H. Yao, Review on the current status of the co-combustion technology of organic solid waste (OSW) and coal in China, Energy Fuel 34 (2020) 15448–15487, https://doi.org/10.1021/acs.energyfuels.0c02177.

[4] D. Vamvuka, N. Salpigidou, E. Kastanaki, S. Sfakiotakis, Possibility of using paper sludge in co-firing applications, Fuel 88 (2009) 637–643, https://doi.org/10.1016/j.fuel.2008.09.029.

[5] B. Leckner, F. Lind, Combustion of municipal solid waste in fluidized bed or on grate – a comparison, Waste Manag. 109 (2020) 94–108, https://doi.org/10.1016/j.wasman.2020.04.050.

[6] M. Frankenhaeuser, M. Hiltunen, H. Manninen, J. Palonen, J. Ruuskanen, T. Vartiainen, Emissions from co-combustion of used packaging with peat and coal, Chemosphere 29 (1994) 2057–2066, https://doi.org/10.1016/0045-6535(94)90373-5.

[7] C.R. McGowin, W.C. Howe, Alternate Fuel Cofiring in Fluidized Bed Boilers, 1994, pp. 155–170.

[8] K. Suksankraisorn, S. Patumsawad, P. Vallikul, B. Fungtammasan, A. Accary, Co-combustion of municipal solid waste and Thai lignite in a fluidized bed, Energy Convers. Manag. 45 (2004) 947–962, https://doi.org/10.1016/S0196-8904(03)00187-0.

[9] A. Atimtay, S. Yurdakul, Combustion and co-combustion characteristics of torrefied poultry litter with lignite, Renew. Energy 148 (2020) 1292–1301, https://doi.org/10.1016/j.renene.2019.10.068.

[10] X. Liu, M. Chen, Y. Wei, Assessment on oxygen enriched air co-combustion performance of biomass/bituminous coal, Renew. Energy 92 (2016) 428–436, https://doi.org/10.1016/j.renene.2016.02.035.

[11] M. Miao, H. Kong, B. Deng, L. Chen, H. Yang, J. Lyu, M. Zhang, Experimental study on N2O and NOx emission characteristics of five high-volatile fuels in bubbling bed combustion, Fuel Process. Technol. 208 (2020) 106517, https://doi.org/10.1016/j.fuproc.2020.106517.

[12] H. Liu, Y. Wang, J. Xue, Y. Zhang, P. Yu, D. Che, Experimental study on combustion, ash fusibility and slagging propensity during co-combustion of organic solid waste and lignite, J. Energy Inst. 106 (2023) 101145, https://doi.org/10.1016/j.joei.2022.11.005.

[13] Y. Gu, H. Cao, W. Liu, X. Lin, T. Zheng, W. Cheng, J. Huang, J. Xu, Impact of co-processing sewage sludge on cement kiln NOx emissions reduction, J. Environ. Chem. Eng. 9 (2021) 105511, https://doi.org/10.1016/j.jece.2021.105511.

[14] Z. Zhao, R. Wang, J. Wu, Q. Yin, C. Wang, Bottom ash characteristics and pollutant emission during the co-combustion of pulverized coal with high mass-percentage sewage sludge, Energy 171 (2019) 809–818, https://doi.org/10.1016/j.energy.2019.01.082.

[15] T. Olugbade, O. Ojo, T. Mohammed, Influence of binders on combustion properties of biomass briquettes: a recent review, Bioenergy Res. 12 (2019) 241–259, https://doi.org/10.1007/s12155-019-09973-w.
[16] W. Żukowski, D. Jankowski, J. Wrona, G. Berkowicz-Płatek, Combustion behavior and pollutant emission characteristics of polymers and biomass in a bubbling fluidized bed reactor, Energy 263 (2023) 125953, https://doi.org/10.1016/j.energy.2022.125953.
[17] R. Yang, C. Ma, G. Chen, Z. Cheng, B. Yan, M. Mansour, Study on NOx emission during corn straw/sewage sludge co-combustion: experiments and modelling, Fuel 285 (2021) 119208, https://doi.org/10.1016/j.fuel.2020.119208.
[18] X. Huo, X. Jia, C. Song, F. Yun, S. Hao, Y. Ding, S. Liu, M. Lei, Investigation of mitigation of nitric oxide emission characteristics and slagging properties from biomass combustion by the additive of coal gangue, J. Environ. Chem. Eng. 10 (2022) 107573, https://doi.org/10.1016/j.jece.2022.107573.
[19] M.U. Degereji, S.R. Gubba, D.B. Ingham, L. Ma, M. Pourkashanian, A. Williams, J. Williamson, Predicting the slagging potential of co-fired coal with sewage sludge and wood biomass, Fuel 108 (2013) 550–556, https://doi.org/10.1016/j.fuel.2012.12.030.
[20] Y. Lin, X. Ma, X. Ning, Z. Yu, TGA–FTIR analysis of co-combustion characteristics of paper sludge and oil-palm solid wastes, Energy Convers. Manag. 89 (2015) 727–734, https://doi.org/10.1016/j.enconman.2014.10.042.
[21] U. Kayahan, S. Özdoğan, Oxygen enriched combustion and co-combustion of lignites and biomass in a 30 kWth circulating fluidized bed, Energy 116 (2016) 317–328, https://doi.org/10.1016/j.energy.2016.09.117.
[22] Y. Wang, Y. Liao, Y. Chen, Y. Bin, X. Ma, Co-combustion of coal and composite board sawdust: combustion behaviors, ash slagging characteristics, and gaseous pollutant emissions and control, Biomass Convers. Biorefinery 14 (2024) 27159–27173, https://doi.org/10.1007/s13399-022-03481-2.
[23] X. Yang, G. Song, Z. Yang, C. Wang, Z. Ji, X. Zhang, Combustion and NOx emission characteristics of coal slime solid waste at different feeding positions, J. Therm. Sci. 32 (2023) 2351–2360, https://doi.org/10.1007/s11630-023-1863-2.
[24] C. Jiang, W. Zhou, H. Bi, Z. Ni, H. Sun, Q. Lin, Co-pyrolysis of coal slime and cattle manure by TG–FTIR–MS and artificial neural network modeling: pyrolysis behavior, kinetics, gas emission characteristics, Energy 247 (2022) 123203, https://doi.org/10.1016/j.energy.2022.123203.
[25] J. Chen, L. Mu, J. Cai, P. Yao, X. Song, H. Yin, A. Li, Pyrolysis and oxy-fuel combustion characteristics and kinetics of petrochemical wastewater sludge using thermogravimetric analysis, Bioresour. Technol. 198 (2015) 115–123, https://doi.org/10.1016/j.biortech.2015.09.011.
[26] Z. Chen, J. Li, S. Guan, Y. Qiao, Z. Yuan, L. Zeng, Z. Li, Kinetics, thermodynamics and gas evolution of atmospheric circulating fluidized bed coal gasification fly ash combustion in air atmosphere, Fuel 290 (2021) 119810, https://doi.org/10.1016/j.fuel.2020.119810.
[27] J. Li, S. Fan, X. Zhang, Z. Chen, Y. Qiao, Z. Yuan, Z. Li, Investigation on co-combustion of coal gasification fine ash and raw coal blends: thermal conversion, gas pollutant emission and kinetic analyses, Energy 246 (2022) 123368, https://doi.org/10.1016/j.energy.2022.123368.
[28] A. Khan, S.R. Naqvi, A.A. Zorpas, D. Juchelková, I. Ali, Thermokinetic study of tannery sludge using combustion and pyrolysis process through non-isothermal thermogravimetric analysis, Sustain. Chem. Pharm. 41 (2024) 101719, https://doi.org/10.1016/j.scp.2024.101719.
[29] Z. Ni, Y. Zhang, X. Liu, H. Shi, Y. Yao, J. Tian, P. Hu, L. He, Q. Lin, L. Liu, Co-combustion of sewage sludge with corn stalk based on TG-MS and TG-DSC: gas products, interaction mechanisms, and kinetic behavior, Energy 308 (2024) 132747, https://doi.org/10.1016/j.energy.2024.132747.
[30] V. Šatava, Mechanism and kinetics from non-isothermal TG traces, Thermochim. Acta 2 (1971) 423–428, https://doi.org/10.1016/0040-6031(71)85018-9.
[31] G. Wang, J. Zhang, J. Shao, Z. Liu, G. Zhang, T. Xu, J. Guo, H. Wang, R. Xu, H. Lin, Thermal behavior and kinetic analysis of co-combustion of waste biomass/low rank coal blends, Energy Convers. Manag. 124 (2016) 414–426, https://doi.org/10.1016/j.enconman.2016.07.045.
[32] S. Hu, X. Ma, Y. Lin, Z. Yu, S. Fang, Thermogravimetric analysis of the co-combustion of paper mill sludge and municipal solid waste, Energy Convers. Manag. 99 (2015) 112–118, https://doi.org/10.1016/j.enconman.2015.04.026.
[33] S. Sun, D. Xu, Y. Liang, G. Jiang, Y. Diao, X. Gong, B. Wang, Effect of temperature, oxygen concentration, and CaO addition on SO2 and NOx emissions during oxygen-fuel combustion of municipal sludge, J. Energy Inst. 105 (2022) 424–432, https://doi.org/10.1016/j.joei.2022.10.012.
[34] A. Tomita, Suppression of nitrogen oxides emission by carbonaceous reductants, Fuel Process. Technol. 71 (2001) 53–70, https://doi.org/10.1016/S0378-3820(01)00136-9.
[35] P.-S. Li, Y. Hu, W. Yu, Y.-N. Yue, Q. Xu, S. Hu, N.-S. Hu, J. Yang, Investigation of sulfur forms and transformation during the co-combustion of sewage sludge and coal using X-ray photoelectron spectroscopy, J. Hazard. Mater. 167 (2009) 1126–1132, https://doi.org/10.1016/j.jhazmat.2009.01.115.
[36] S. Zhu, J. Hui, Q. Lyu, Z. Ouyang, X. Zeng, J. Zhu, J. Liu, X. Cao, X. Zhang, H. Ding, Y. Liu, Experimental study on pulverized coal swirl-opposed combustion preheated by a circulating fluidized bed. Part A. Wide-load operation and low-NOx emission characteristics, Energy 284 (2023) 128573, https://doi.org/10.1016/j.energy.2023.128573.
[37] Z. Gong, L. Wang, Z. Wang, Z. Wang, Y. Xu, F. Sun, Z. Sun, Z. Liu, L. Zhu, Experimental study on combustion and pollutants emissions of oil sludge blended with microalgae residue, J. Energy Inst. 91 (2018) 877–886, https://doi.org/10.1016/j.joei.2017.10.001.
[38] L. Li, L. Duan, Z. Yang, Y. Wang, W. Xiang, Experimental study on in-situ denitration using catalyst in fluidized bed reactor, Fuel Process. Technol. 216 (2021) 106742, https://doi.org/10.1016/j.fuproc.2021.106742.
[39] J. Cheng, J. Zhou, J. Liu, Z. Zhou, Z. Huang, X. Cao, X. Zhao, K. Cen, Sulfur removal at high temperature during coal combustion in furnaces: a review, Prog. Energy Combust. Sci. 29 (2003) 381–405, https://doi.org/10.1016/S0360-1285(03)00030-3.
[40] J. Hu, Y. Yan, Y. Song, J. Liu, F. Evrendilek, M. Buyukada, Catalytic combustions of two bamboo residues with sludge ash, CaO, and Fe2O3: bioenergy, emission and ash deposition improvements, J. Clean. Prod. 270 (2020) 122418, https://doi.org/10.1016/j.jclepro.2020.122418.
[41] F. Okasha, Enhancing sulphur self-retention by building-in CaO in straw–bitumen pellets, Fuel Process. Technol. 88 (2007) 401–408, https://doi.org/10.1016/j.fuproc.2006.12.001.
[42] Y. Rahib, T. Boushaki, B. Sarh, J. Chaoufi, Combustion and pollutant emission characteristics of argan nut shell (ANS) biomass, Fuel Process. Technol. 213 (2021) 106665, https://doi.org/10.1016/j.fuproc.2020.106665.